第 27 卷第 4 期 无 机 化 学 学 报 Vol.27 No.4
2011 年 4 月 CHINESE JOURNAL OF INORGANIC CHEMISTRY 752-758

ZnO 微结构调控及其光学性能的研究

刘海霞 黄柏标* 王泽岩 秦晓燕 张晓阳 俞娇仙
(山东大学晶体材料国家重点实验室,济南 250100)

摘要: 氧化锌不同形貌的合成与控制可以通过一个简单的溶剂热反应来实现,其中乙醇作溶剂,酒石酸做添加剂。通过控制酒石酸的加入量,可以有效地控制 ZnO 的形貌、尺寸以及到更复杂结构的转变。同时提出了不同形貌 ZnO 可能的生长机制,并利用 FTIR 谱进一步证实了酒石酸对 ZnO 生长的影响。另外,由光致发光光谱可以看出,不同的 ZnO 形貌,发光性能会有所不同,总体上说,所得 ZnO 的发光区域主要集中在紫光波段和橙光波段。

关键词: 氧化锌; 微结构; 机理; 光学性能
中图分类号: O614.24+1 **文献标识码**: A **文章编号**: 1001-4861(2011)04-0752-07

Synthesis and Optical Properties of Assembly-Controlled ZnO Structures

LIU Hai-Xia HUANG Bai-Biao* WANG Ze-Yan QIN Xiao-Yan ZHANG Xiao-Yang YU Jiao-Xian
(*State Key Laboratory of Crystal Materials, Shandong University, Jinan* 250100, *China*)

Abstract: A facile solvothermal synthesis of ZnO architectures has been developed using ethanol as solvent and tartaric acid as the additive. The variational quantities of tartaric acid controlled the ZnO morphology and shape as well as the self-assembly of ZnO crystals into complex architectures. Possible growth mechanisms of obtained ZnO with different morphologies were proposed. The influence of tartaric acid to ZnO growth was further indicated by FTIR spectra. In addition, the photoluminescence (PL) properties of these ZnO samples were investigated at room temperature, which indicated that the ZnO morphology could influence its optical property. On the whole, the fluorescence was violet emission and orange emission primarily.

Key words: zinc oxide; microstructures; mechanism; optical property

Introduction

Nano- and micro-structured materials have attracted increasing interests from chemists and materials scientists in recent years [1-3]. The design, fabrication and modification of hierarchical structures with controllable morphologies remain a great challenge. Zinc oxide (ZnO) is an important n-type semiconductor with a wide direct band gap (3.37 eV) and a large exciton binding energy (60 meV). Because of its excellent thermal and chemical stability, ZnO has been investigated for applications in many areas, such as photoelectronics, photocatalysis, field emission and sensors[4-8]. Likewise, the properties of ZnO are closely related to its structures, such as morphologies, sizes, aspect ratios or surface architectures, etc[9-11]. Up to now, ZnO with different structures and morphologies have been synthesized, including ZnO nanowires, nanorods, nanotubes, branches, tetrapods and microtorches, etc[12-19]. Among the various methods[12-23], wet chemical approach is regarded as one of the best way to synthesize ZnO materials without the demand of

收稿日期:2010-11-10。收修改稿日期:2010-12-16。
973 国家重点基础研究项目(No.2007CB613302);国家自然科学基金(No.20973102,51021062,51002091)资助项目。
*通讯联系人。E-mail: bbhuang@sdu.edu.cn,Tel:0531-88364449

special equipment, complex process or high temperature. With better control over size and morphology, wet chemical method used for ZnO synthesis has been reported by many groups [24-29]. Recently, organic molecules, such as PSS, PEG, TEA, etc., have been widely employed as surfactant to construct ZnO hierarchical arthitectures [30-33]. Organic acid, for its complexation with metal ions, is one of the rising modifiers in the synthesis of ZnO. Cho et al. have studied the effect of *L*(+)-ascorbic acid (vitamin C) on the formation of ZnO crystals under weak acidic to alkaline conditions [34]. The amino acid histiduine has been introduced as the directing and assembling agent and a series of ZnO hierarchical architectures have been developed, including prismlike, flowerlike and non-crystalline hollow microspheres[35].

In this paper, we synthesized ZnO micro-crystals by a simple solvothermal method with the addition of tartaric acid. Different from the traditional ZnO preparation method, where the precursor solutions are usually alkaline in favor of the formation of $Zn(OH)_4^{2-}$ growth units, there is not any alkaline matter used during the whole synthetic process. By controlling the addition of tartaric acid, a series of ZnO samples with different morphologies and sizes have been obtained. Tartaric acid was regarded to play an important role on the ZnO morphology. The room-temperature photoluminescence properties were also systematically investigated.

1 Experimental

All the reagents and solvents were analytical grade and used without any further purification. In a typical solvothermal process, the precursor solution was prepared by dissolving 14.85 g zinc nitrate hexahydrate ($Zn(NO_3)_2 \cdot 6H_2O$) into 100 mL absolute ethanol under vigorous magnetic stirring. After $Zn(NO_3)_2 \cdot 6H_2O$ dissolved completely, 1.8 g tartaric acid was added to the above solution under continuous stirring to form a clear solution. After 30 min stirring, the mixture was transferred to the autoclave and was kept at 160 ℃ for 4 h in oven, including 0.5 h for heating up. The final products were obtained after washed with deionized water and ethanol for several times, and dried at 70 ℃ in air. Under identical conditions, a series of experiments were also carried respectively with tartaric acid amounts changed (1.8, 1.2, 0.8, 0.6, 0.4, 0.1 g).

The morphologies of ZnO crystals were characterized by using scanning electron microscopy (SEM, Hitachi S4800) with an accelerating voltage of 5 kV and high-resolution transmittance electron microscopy (HR-TEM, JEOL JEM-2100; 200 kV). X-ray diffraction (XRD) analysis was performed with a Bruker AXS D8 advance powder diffractometer with Cu *Kα* radiation. The products were investigated by using Fourier transform infrared (FTIR) spectroscopy (Nexus 670, Thermo Nicolet, USA) with smart iTR accessory. Photoluminescence (PL) measurements were carried out for the as-prepared ZnO different structures at room temperature with a luminescence spectrometer (Edinbergh FLS 920) using 325 nm as the excitation wavelength.

2 Results and discussion

The reacti on parameters including the reactant concentration, temperature and pH value, play crucial roles in controlling the size and morphology of the products. In our studies, the morphology and phase structure of the as-synthesized ZnO could be facilely turned just by changing the amount of tartaric acid, while the other conditions remained unchanged.

When tartaric acid was present in high addition as 1.8 g, the mask-like ZnO was obtained with a diameter of 10~20 μm as shown in Fig.1a~b. Because the concentration of tartaric acid was so high, there were many organic acid molecules and ions around Zn^{2+} ions, and the generated ZnO growth unit was the center in a small region. In this case, tartaric acid acted as a surface active agent around ZnO nucleus, which made the surrounding dissociative Zn^{2+} ions could crystallize in a slow rate. In this way, the central ZnO nucleus could grow into big crystals at a low speed gradually. With the addition of tartaric acid decreased to 1.2 g, ZnO flowers with an average diameter of 2 μm were synthesized (Fig.1c). From the enlarged image shown in Fig.1d, we could see that each flower was made up of directional nanorods. The perfectly aligned lattice

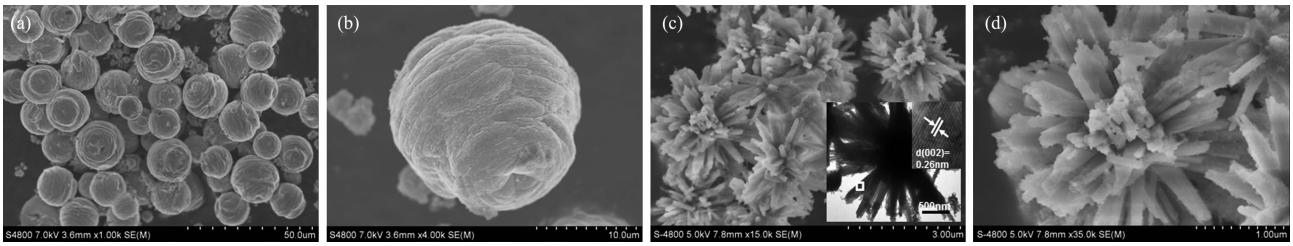

Fig.1 (a) SEM image of mask-like ZnO architectures grown with 1.8 g tartaric acid; (b) The high-magnification image of ZnO mask; (c) SEM image of flower-like ZnO architectures grown with 1.2 g tartaric acid. The inset shows TEM image and an enlargement of the sample area in white frame; (d) The high-magnification image of ZnO flower

planes, as shown in the lower-right inset of Fig.1c, provided strong evidence for the well-crystallized architecture of ZnO flowers. Each highly crystalline rod of ZnO flowers had a spacing distance of about 0.26 nm, corresponding to the interspacing of the (002) planes, which was the routine direction for one dimensional ZnO growth. As the tartaric acid decreased, the Zn^{2+} ions increased relatively, but still acted as the centers with organic matter surrounded in small regions. There were more centers to the nucleation, and these ZnO nucleuses grew along one-dimensional direction. With the reaction time prolonged, plenty of ZnO nanorods appeared and constituted the ZnO flowers through static adsorption of ZnO polarity. From the above discussion, when tartaric acid was present with a large amount (1.8 g, 1.2 g), the organic molecules could surround the ZnO nucleus and control its surface growth, which influenced the ZnO morphologies as surface active agents.

When tartaric acid deceased to 0.8 g, ZnO spheres with thorns formed gradually, whose diameters were about 1 μm (Fig.2a~b). For TEM analysis, these big spheres had been crushed into small crystals as shown in Fig.2c. The HRTEM image corroborated the ZnO spheres were actually composed of nanometer-sized ZnO units, arranged along (002) direction in a specific way, as displayed in Fig.2d. The diffraction rings shown in the inset of Fig.2d, resulted from the SAED analysis on the edge of the ZnO sphere, further indicated that the obtained sphere was polycrystalline ZnO. In this condition, the acid/Zn^{2+} molar ratio became much lower and tartaric acid molecules, instead of the ZnO units, became the centers in a small region. Correspondingly, there were plenty of Zn^{2+} ions gathering around the central giant molecule. In this way, tartaric acid played

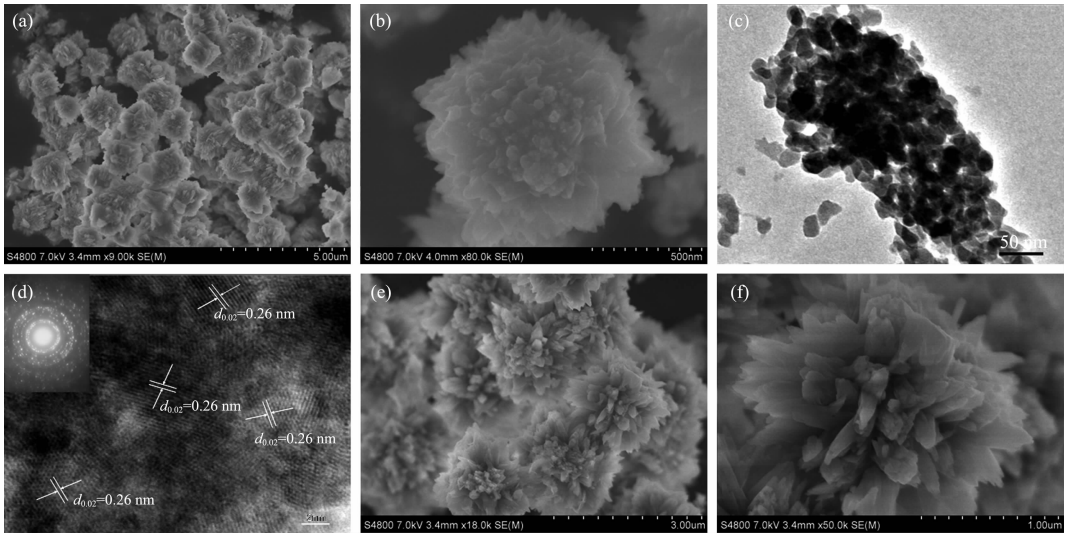

Fig.2 (a) SEM image of ZnO spheres with thorns grown with 0.8 g tartaric acid. (b) The high-magnification image of ZnO sphere. (c) and (d) showed TEM image and TRTEM image of the crushed sphere, respectively. The inset in panel d shows the SAED pattern of the sample. (e) SEM image of ZnO blossoms grown with 0.6 g tartaric acid. (f) The high-magnification image of ZnO blossom

a morphology-directing role in ZnO growth. Later on, tartaric acid molecules overflowed from inside and the surrounding Zn^{2+} ions continue to crystallize, which finally formed the ZnO spheres and the superfluous ZnO units crystallized into the peripheral thorns on the surface. When the addition of tartaric acid was 0.6 g, the relative Zn^{2+} concentration was higher, and the surrounding ZnO units around the central organic molecule congregated to a great extent (Fig.2e~f). The former thorn (Fig.2a) of the surface became a prominent petal with thick bottom and thin top. The whole morphology liked a blossom with pronounced petals, and each petal had a length of ~300 nm.

With the present tartaric acid decreased to 0.4 g, durian-like ZnO was formed as shown in Fig.3a~b. The durian had a size of 6~8 μm and there were obvious cracks from the inside to outside on the durian. The growth mechanism was similar to the former spheres and blossoms, and tartaric acid was still the center and the template. But because the amount of tartaric acid was reduced, the small quantity of organic molecules did not have enough power to overflow from inside rapidly until the last stage that all the Zn^{2+} ions had crystallized. Then it was not surprising that there were some cracks on the surface of durian-like ZnO. From the enlarged image (Fig.3b), we could see that the surface of durian was composed with nanosheets that came from the superfluous ZnO units as well. When tartaric acid was changed to 0.1 g, ZnO balls were generated (Fig.3c~d). The balls were loose and constituted with small nanocrystals. Each ball had a diameter of 2 μm and each composed crystal had a nanoscale size. Tartaric acid, which acted still as the morphology-directing agent, was added with a little amount, so the organic molecules could overflow through the loosen structure and the cracks did not form anymore.

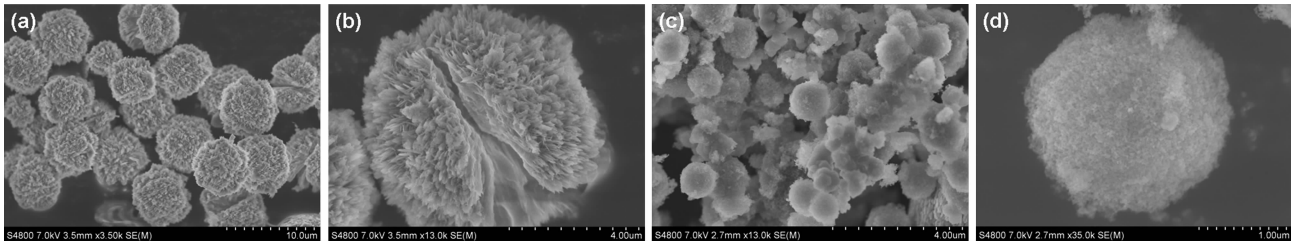

Fig.3 (a) SEM image of durian-like ZnO architectures grown with 0.4 g tartaric acid. (b) The high-magnification image of ZnO durian. (c) SEM image of ZnO spheres composed of small crystals grown with 0.1 g tartaric acid. (d) The high-magnification image of ZnO sphere

A schematic diagram of the possible formation mechanism of the various ZnO has been shown in Fig.4. Moreover, the initial formation reactions of ZnO crystals in the ethanol have been studied profoundly in the literature[36] as follows:

$$4CH_3CH_2OH+NO_3^- \rightarrow 4CH_3CHO+NH_3\uparrow+OH^-+2H_2O \quad (1)$$

$$Zn^{2+}+2OH^- \rightarrow ZnO+H_2O \quad (2)$$

From the above formula we can see that absolute ethanol is the solution as well as the reactant, which reacts with the nitrate and produces the original OH^- ions. This explained the ZnO formation in the neutral or weak acidic environment.

Fig.5 shows the typical XRD patterns of the obtained ZnO architectures. The six ZnO structures have similar XRD patterns, except for relative peak intensities, due to their random orientation. All diffraction peaks can be indexed to wurtzite structured

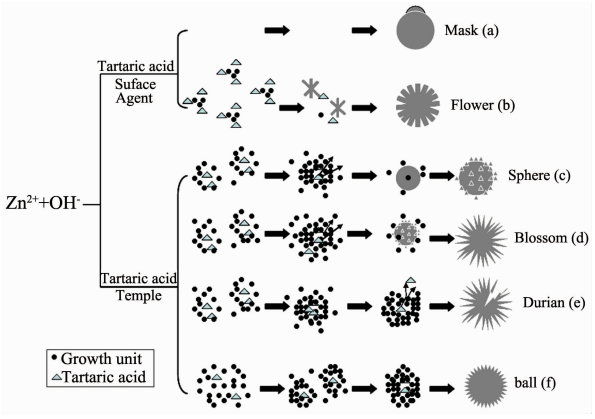

(a) masks; (b) flowers; (c) spheres; (d) blossoms; (e) durians; (f) balls

Fig.4 Schematic diagram of the proposed formation processes of the different ZnO structures

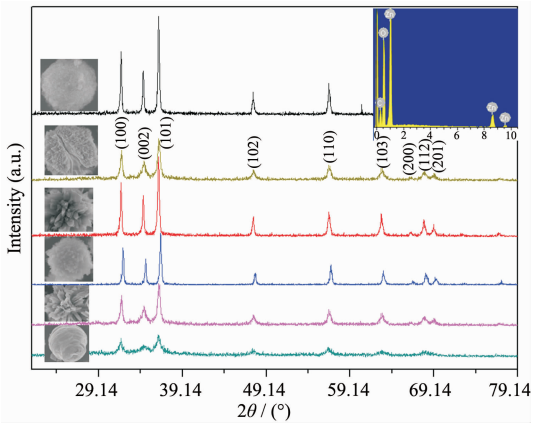

Fig.5 XRD patterns of the ZnO architectures synthesized with different concentrations of tartaric acid; the inset is EDS pattern

ZnO (space group $P6_3mc$) with cell parameters a=0.325 nm and c=0.521 nm, which is in good agreement with the literature values (JCPDS card, No. 36-1451). No peaks of other impurities are detected in the patterns, suggesting that only single-phase ZnO samples were formed. And the insert EDS pattern further indicates that the samples were composed of only Zn and O; the C signal was attributed to the carbonous tape used.

The influence of tartaric acid molecules to the ZnO morphologies has been proved by FTIR spectra (Fig.6). Because the spectra of some simples are similar and coincident nearly, so we have selected several representative IR spectra. The spectra of flowerlike, durian-like and mask-like ZnO are shown in Fig.6a~c, respectively. The peaks at ca. 3 450 and 1 620 cm^{-1} should be derived from the stretching vibrations and deformation vibrations of -OH group of atmospheric water on the ZnO surfaces, respectively. Compared with Fig.6d, abundant of peaks marked specially from 700 to 1 500 cm^{-1} in Fig.6a~c are in accordance with pure tartaric acid, especially at the peak centered at 1 130 and 1 316 nm marked with the symbol (^). It implies that tartaric acid molecules are adsorbed on the surface of ZnO crystals and the ZnO fabrication should have been influenced by tartaric acid largely. From the partial enlarged detail in the image, we can see that there is a peak at 1 086 cm^{-1} in the spectrum of mask-like ZnO in consistent with pure tartaric acid, which is absent in curve a and b. The same occurs in the peak of 1 409 cm^{-1}. This implied that tartaric acid played a more important role on the formation of mask-like ZnO. The reason was that in the process of mask-like ZnO fabrication, tartaric acid was added with a bigger amount and most of the molecules were adsorbed on the surface of ZnO crystals due to their roles of surface active agent.

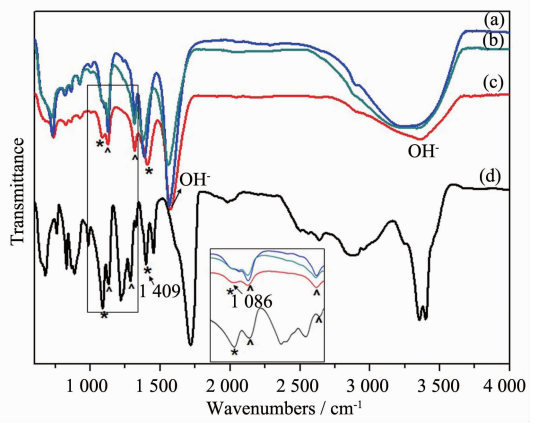

(a) the flower-like ZnO; (b) the durian-like ZnO; (c) the mask-like ZnO. (d) IR spectrum of pure tartaric acid

Fig.6 FTIR spectra of the ZnO architectures

It′ s well known that different peak luminous wavelength of ZnO crystals could be induced by several factors, such as morphologies, crystal defects and impurity levels. The room-temperature PL spectra of as-prepared ZnO structures were obtained with an excitation wavelength of 325 nm, shown in Fig.7. Its clear that there are obvious peaks centered at ca. 450 nm in most samples except b, and belong to the violet emission. The violet emission could be ascribed to the red shift of the band edge emission because of the

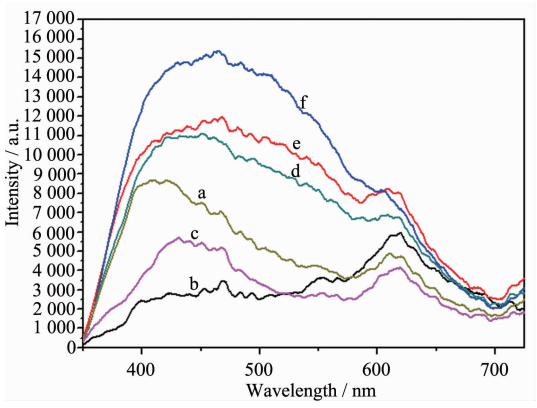

(a) masks; (b) flowers; (c) spheres; (d) blossoms; (e) durians; (f) balls

Fig.7 Room-temperature PL of the ZnO architectures synthesis with tartaric acid variational

formation of surface states below the conduction band[37]. The similar result that the strongest emission existed in visible region has been observed in Wang′s work[38] and the origin was also contributed to the surface adsorption through experimental confirmation, which was in good accordance with our theory. Among these curves, with a decreasing addition of tartaric acid in the solvents, the PL spectra show a gradual red shift from 400 nm to 460 nm in the peak position of the highest peaks, which could be due to different surface states in different samples. What′s more, there are obvious orange emission centered at ca. 618 nm in curve a, b and c. The orange emission as deep level emission was associated with the defect-related transitions through previous studies [39-40]. Huang et al. further proved that the interstitial oxygen ions caused a strong orange emission finally [41]. In addition, with little violet emission, sample b shows a more intense orange emission than sample a and c. The specific causes need much more research in the future. In sum the controllable morphologies could affect the optical characters of the ZnO with various peak positions and different intensities.

3 Conclusions

ZnO micro stru ctures with different morphologies were prepared by a simple solvothermal synthesis with tartaric acid as an additive. Tartaric acid with different quantity has been used as a shape modifier and proved to be efficient at controlling the ZnO architectures. The possible action mechanisms of tartaric acid in the high and low concentration have been proposed respectively. The IR spectra indicated that the tartaric acid molecules were absorbed on the surface of ZnO crystals and they were more effective when they played as a surface agent. The PL spectra showed that the obtained ZnO had strong visible emissions and the morphologies of as-prepared ZnO could influence their optical properties.

Ack nowledgement: This work was financially supported by research grants from the National Basic Research Program of China (No.2007CB613302) and the National Natural Science Foundation of China (No.20973102, 51021062 and 51002091).

References:

[1] Yang J, Qi L, Lu C, et al. *Angew. Chem. Int. Ed*., **2005**,**44**: 598-603

[2] Yan C, Xue D. *J. Phys. Chem. B*, **2005**,**109**:12358-12361

[3] Goldberger J, He R, Zhang Y, et al. *Nature*, **2003**,**422**:599-602

[4] Keis K, Vayssieres L, Lindquist S E, et al. *Nanostruct. Mater.*, **1999**,**12**:487-490

[5] Schrier J, Demchemko D O, Wang L W. *Nano Lett*., **2007**,**7**: 2377-2382

[6] Tian N, Zhou Z Y, Sun S G, et al. *Science*, **2007**,**316**:732-735

[7] Arnold M S, Avouris P, Pan Z W, et al. *J. Phys. Chem. B*, **2003**, **107**:659-663

[8] DENG Chong-Hai(邓崇海), HU Han-Mei(胡寒梅), HUANG Xian-Huai(黄显怀). *Chinese J. Inorg. Chem.*(*Wuji Huaxue Xuebao*), **2009**,**25**:469-473

[9] Zhang J, Sun L, Yin J, et al. *Chem. Mater*., **2002**,**14**:4172-4177

[10]Zhao Q, Zhang H Z, Zhu Y W, et al. *Appl. Phys. Lett.*, **2005**, **86**:203115(3 pages)

[11]GONG Hai-Yan(龚海燕), LI Xiao-Hong(李小红), ZHANG Zhi-Jun(张治军). *Chinese J. Inorg. Chem.*(*Wuji Huaxue Xuebao*), **2006**,**22**:426-430

[12]Vayssieres L. *Adv. Mater*., **2003**,**15**:464-466

[13]Wang Z Y, Huang B B, Qin X Y, et al. *Mater. Lett*., **2009**, **63**:130-132

[14]She G W, Zhang X H, Shi W S, et al. *Electrochem. Commun*., **2007**,**9**:2784-2788

[15]Lao J Y, Wen J G, Ren Z F. *Nano Lett*., **2002**,**2**:1287-1291

[16]HAN Dong(韩冬), ZHANG Shu-Chao(张树朝). *Acta Phys.-Chim. Sin.*(*Wuli Huaxue Xuebao*), **2008**,**24**:539-542

[17]DING Shi-Wen(丁士文), ZHANG Shao-Yan(张绍岩), LIU Shu-Juan(刘淑娟), et al. *Chinese J. Inorg. Chem.* (*Wuji Huaxue Xuebao*), **2002**,**18**:1015-1019

[18]Yu W, Li X, Gao X. *Cryst. Growth Des*., **2005**,**5**:151-155

[19]Xu F, Lu Y, Xie Y, et al. *Mater. Des*., **2009**,**30**:1704-1711

[20]Pradhan B, Batabyal S K, Pal A J. *Sol. Energ. Mater. Sol. Cells*., **2007**,**91**:769-773

[21]Rout C S, Raju A R, Govindaraj A, et al. *J. Nanosci. Nanotechnol.*, **2007**,**7**:1923-1929

[22]Wan Q, Li Q H, Chen Y J, et al. *Appl. Phys. Lett*., **2004**,**84**: 3654-3656

[23]Law M, Greene L E, Johnson J C, et al. *Nat. Mater*., **2005**,**4**:

455-459

[24]Ursaki V V, Rusu E V, Sarua A, et al. *Nanotechnology*, **2007**,**18**:215705(8pages)

[25]LI Bo(李博), CUI Yu-Ming(崔玉明), LIU Lei(刘磊), et al. *Chinese J. Inorg. Chem.* (*Wuji Huaxue Xuebao*), **2009**,**25**: 2077-2082

[26]Xu F, Yu K, Li G D, et al. *Nanotechnology*, **2006**,**17**:2855-2859

[27]Jiang P, Zhou J J, Fang H F, et al. *Adv. Funct. Mater.*, **2007**,**17**:1303-1310

[28]Gao X, Li X, Yu W. *J. Phys. Chem. B*, **2005**,**109**:1155-1161

[29]Liang J, Liu J, Xie Q, et al. *J. Phys. Chem. B*, **2005**,**109**: 9463-9467

[30]Liu J P, Huang X T, Sulieman K M, et al. *J. Phys. Chem. B*, **2006**,**110**:10612-10618

[31]Mo M S, Yu J C, Zhang L Z, et al. *Adv. Mater.*, **2005**,**17**: 756-760

[32]Cheng B, Wang X F, Liu L Y, et al. *Mater. Lett.*, **2008**,**62**: 3099-3102

[33]Mohajerani M S, Mazloumi M, Lak A, et al. *J. Cryst. Growth*, **2008**,**310**:3621-3625

[34]Cho S, Jeong H, Park D H, et al. *CrystEngComm.*, **2010**,**12**: 968-976

[35]Wu Q, Chen X, Zhang P, et al. *Cryst. Growth Des.*, **2008**,**8**: 3010-3018

[36]Sun X, Qiu X, Li L, et al. *Inorg. Chem.*, **2008**,**47**:4146-4152

[37]Ghoshal T, Kar S, Chaudhuri S. *Cryst. Growth Des.*, **2007**, 7:136-141

[38]Wang F, Cao L, Pan A, et al. *J. Phys. Chem. C*, **2007**,**111**: 7655-7660

[39]Pol V G, Calderon-Moreno J M, Thiyagarajan P. *Langmuir*, **2008**,**24**:13640-13645

[40]Tam K H, Cheung C K, Leung Y H, et al. *J. Phys. Chem. B*, **2006**,**110**:20865-20871

[41]Wang Z Y, Huang B B, Liu X J, et al. *Mater. Lett.*, **2008**, **62**:2637-2639